OPEN ACCESS

*International*
*Journal*
*Of Modern Engineering Research (IJMER)*

# Embedded Controlled Multiple Output Boost Converter

Brunda N.[1], K. J. Madhuselvi[2]
[1, 2] *(P.G (PE&D) student, Asst.Professor, Department of EEE, Dhanalakshmi Srinivasan Engineering College, Perambalur-12)*

***Abstract:*** *This project "Embedded Controlled Multiple Output Boost Converters" is composed of a high-efficiency single-input multiple-output (SIMO) dc-dc converter. The proposed converter can boost the voltage of a low-voltage input power source to a controllable high-voltage dc bus and middle-voltage output terminals. In this project, a coupled-inductor based dc-dc converter scheme utilizes single switch with the properties of voltage clamping and soft switching. DC-DC multi-output boost (MOB) converter shares its total output between different series of output voltages for low-and high-power applications. As a result, the objectives of high-efficiency power conversion with various output voltage levels can be obtained and verified through simulation using Matlab-simulink.*
***Index terms:*** *Coupled inductor, high-efficiency power conversion, single-input multiple (SIMO) converter, soft switching, voltage clamping.*

## I. Introduction

DC-DC converters with step voltage ratio are usually required in many industrial applications. The conventional boost converters cannot provide such a high dc voltage gain, even for an extreme duty cycle. In order to increase the conversion efficiency and voltage gain, many modified boost converter topologies have been investigated in the past decade. Although voltage-clamped techniques are manipulated in the converter design to overcome the severe reverse- recovery problem of the output diode in high voltage applications, there still exists overlarge switch voltage stresses and the voltage gain is limited by the turn-on time of the auxiliary switch. The output voltage of the fuel cell decreases as the output power increases, and it is varied easily with respect to the load variations [1]-[2].As the load decreases, the difference of the conduction losses reduces sharply, so the switching loss can be a dominant factor in light-load conditions [3].In addition to the FC stack itself, some other auxiliary components, such as the balance of plant (BOP) including an electronic control board, an air compressor, and a cooling fan, are required for the normal work of an FC generation system [4]-[5].

The proposed converter has lower efficiency at heavy –load conditions and conduction loss in the converter can be higher [6].In other words, the generated power of the FC stack also should satisfy the power of the BOP.Thus, various voltage levels should be required in the power converter of an FC generation system [7].It contains the dissipative RCD snubber and it does not employ the synchronous rectification techniques to reduce the conduction losses on the secondary-side rectifiers [8]. However, over three switches for one output were required. This scheme is only suitable for the low output voltage and power application, and its power conversion is generated due to the operation of hard-switching[9]-[10].Unfortunately, over two switches for one output were required, and its control scheme was complicated. Besides, the corresponding output power cannot supply for individual loads independently [11]-[12].This combination scheme with three full-bridge converters is more complicated, so that the objective of high-efficiency power conversion is difficult to achieve, and its cost is inevitably increased[13]-[14]. It suffers from low voltage gain due to the absence of coupled inductor [15].Voltage clamping and soft switching properties are not used, which increases the conduction and switching losses [16].

This study presents a SIMO converter with coupled inductor. As for the coupled inductor in the proposed SIMO converter, it is designed with lower turns in the primary side to reduce the coil loss, and works well for the application with large input current. It uses only one power switch to overcome the objectives of high-efficiency power conversion, high-step-up ratio and different output voltage levels. The techniques of soft switching and voltage clamping are adopted to reduce the switching and conduction loses. Additionally, the problems of the stray inductance energy and reverse-recovery currents within diodes in the conventional boost converter also can be solved. The output voltage of the high-voltage dc bus can be stably controlled by a simple proportional integral (PI) control.

## II. Proposed Converter Configuration

The motivation of this study is to design a single-input multiple-output (SIMO) converter for increasing the conversion efficiency and voltage gain, reducing the control complexity, and saving the manufacturing cost. The system configuration of the proposed high-efficiency SIMO converter topology to generate three different voltage levels from a single-input power source is depicted in Fig. 1. This SIMO converter contains five parts including a low-voltage-side circuit (LVSC), a clamped circuit, a middle-voltage circuit, an auxiliary circuit, and a high-voltage-side circuit (HVSC). The major symbol representations are summarized as follows. $V_{FC}$ ($i_{FC}$) and $V_{O1}$ ($i_{O1}$ ), $V'_{O1}$ ($i'_{O1}$ ), denote the voltages (currents) of the input power source and the output load at the LVSC and the auxiliary circuit, respectively; $V_{O2}$ and $i_{O2}$ are the output voltage and current in the HVSC. $C_{FC}$, $C_{O1}$,$C'_{O1}$, and $C_{O2}$ are the filter capacitors at the LVSC, the auxiliary circuit, and the HVSC, respectively;$C1$ and $C2$ are the clamped and middle-voltage capacitors in the clamped and middle-voltage circuits, respectively. *LP* and *LS* represent individual inductors in the primary and secondary sides of the coupled inductor $T_r$ , respectively, where the primary side is connected to the input power source; $L_{aux}$ is the auxiliary circuit inductor. The main switch is expressed as $S_1$ in the LVSC; the equivalent load in the auxiliary circuit is represented as $R_{O1}$, $R_{O'1}$, and the output load is represented as $R_{O2}$ in the HVSC.

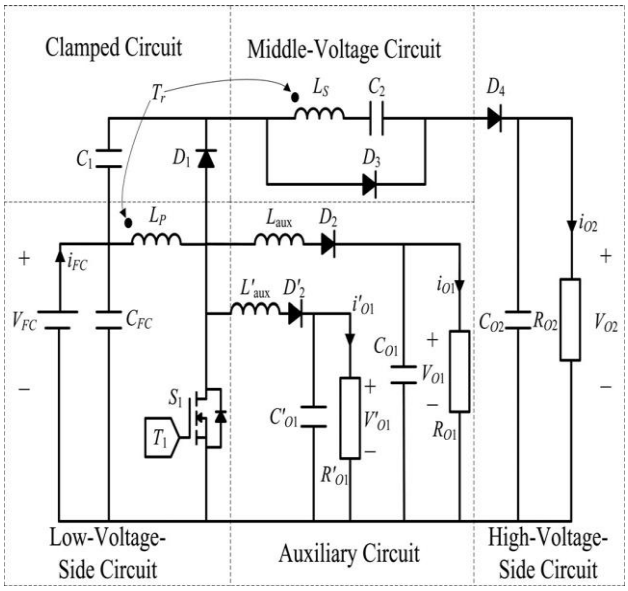


Fig.1.Proposed Converter

$$N = \frac{N_2}{N_1} \qquad (1)$$

$$K = \frac{L_{mp}}{(L_{kp} + L_{mp})} = \frac{L_{mp}}{L_p} \qquad (2)$$

Where $N_1$ and $N_2$ are the winding turns in the primary and secondary sides of the coupled inductor $T_r$ . Because the voltage gain is less sensitive to the coupling coefficient and the clamped capacitor $C_1$ is appropriately selected to completely absorb the leakage inductor energy [13], the coupling coefficient could be simply set at one ($k$ = 1) to obtain $L_{mp} = L_P$ via (2). In this study, the following assumptions are made to simplify the converter analyses: 1) The main switch including its body diode is assumed to be an ideal switching element; and 2) The conduction voltage drops of the switch and diodes are neglected.

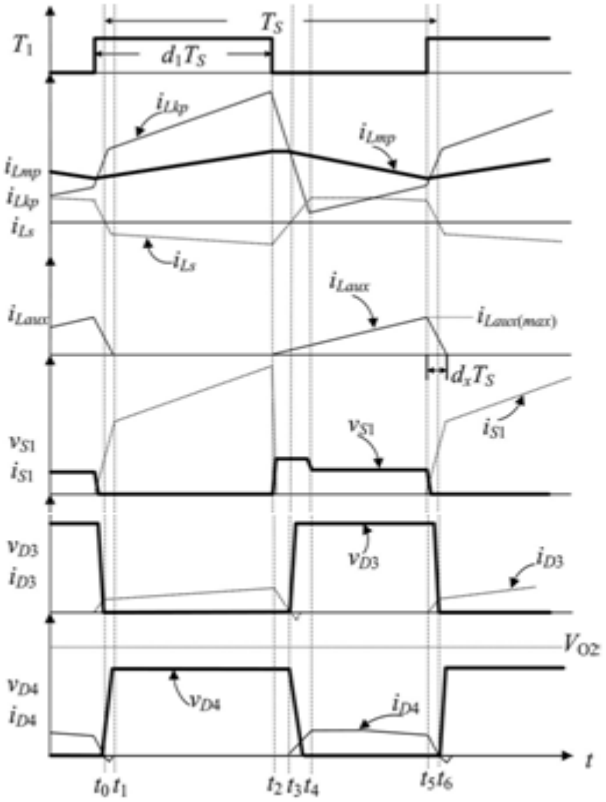


Fig.2.Operating Modes

## III. Principle of Operation

The characteristic waveforms are depicted in Fig. 2.Mode 1 ($t_0$ –$t_1$): In this mode, the main switch $S_1$ was turned ON for a span, and the diode $D_4$ turned OFF. Because the polarity of the windings of the coupled inductor $T_r$ is positive, the diode $D_3$ turns ON. The secondary current $i_{Ls}$ reverses and charges to the middle voltage capacitor $C_2$. When the auxiliary inductor $L_{aux}$ releases its stored energy completely, and the diode $D_2$ turns OFF, this mode ends. Mode 2 ($t_1$ –$t_2$): At time t = $t_1$, the main switch $S_1$ is persistently turned ON. Because the primary inductor $L_P$ is charged by the input power source, the magnetizing current $i_{Lmp}$ increases gradually in an approximately linear way. At the same time, the secondary voltage $v_{Ls}$ charges the middle-voltage capacitor$C_2$ through the diode $D_3$. Although the voltage $v_{Lmp}$ is equal to the input voltage $V_{FC}$ both at modes 1 and 2, the ascendant slope of the leakage current of the coupled inductor ($diL_{kp}$ /dt) at modes 1 and 2 is different due to the path of the auxiliary circuit. Because the auxiliary inductor $L_{aux}$ releases its stored energy completely, and the diode $D_2$ turns OFF at the end of mode 1, it results in the reduction of $diL_{kp}$ /dt at mode.

$$v_{Lmp} = V_{FC} \qquad (3)$$

$$V_{C2} = NV_{FC} \qquad (4)$$

Mode 3 ($t_2$ –$t_3$): At time t = $t_2$, the main switch $S_1$ is turned OFF. When the leakage energy still released from the secondary side of the coupled inductor, the diode $D_3$ persistently conducts and releases the leakage energy to the middle-voltage capacitor $C_2$. When the voltage across the main switch $v_{S1}$ is higher than the voltage across the clamped capacitor $V_{C\ 1}$, the diode $D_1$ conducts to transmit the energy of the primary-side leakage inductor $L_{kp}$ into the clamped capacitor $C_1$. At the same time, partial energy of the primary-side leakage inductor $L_{kp}$ is transmitted to the auxiliary inductor $L_{aux}$, and the diode $D_2$ conducts. Thus, the current $i_{Laux}$ passes through the diode $D_2$ to supply the power for the output load in the auxiliary circuit. When the secondary side of the coupled inductor releases its leakage energy completely, and the diode $D_3$ turns OFF, this mode ends

. $v_{Lmp} = [-\frac{d_1}{1-d_1}]V_{FC}$ (5)

$$V_{C1} = -V_{Lmp} = [\frac{d_1}{1-d_1}]V_{FC} \qquad (6)$$

According to Kirchhoff's voltage law, the output voltage $V_{O2}$ can be obtained as,

$$V_{O2} = V_{FC} + V_{C1} + V_{C2} - v_{Ls} \qquad (7)$$

By using the voltage-second balance, the relation of the average voltage across the secondary winding $V_{Ls}$ to be zero can be expressed by (4) and (7) as

$$(NV_{FC})d_1T_S + (V_{FC} + V_{C1} + V_{C2} - V_{O2})(1 - d_1)T_S = 0 \qquad (8)$$

Mode 4 ($t_3$ –$t_4$): At time t = $t_3$, the main switch $S_1$ is persistently turned OFF. When the leakage energy has released from the primary side of the coupled inductor, the secondary current $i_{LS}$ is induced in reverse from the energy of the magnetizing inductor $L_{mp}$ through the ideal transformer, and flows through the diode $D_4$ to the HVSC. At the same time, partial energy of the primary side leakage inductor $L_{kp}$ is still persistently transmitted to the auxiliary inductor $L_{aux}$, and the diode $D_2$ keeps conducting. Moreover, the current $i_{Laux}$ passes through the diode $D_2$ to supply the power for the output load in the auxiliary circuit.

From (4)–(8), the voltage gain $G_{VH}$ of the proposed SIMO converter from the LVSC to the HVSC can be given as

$$G_{VH} = \frac{V_{O2}}{V_{FC}} = \frac{N+1}{1-d_1} \qquad (9)$$

Mode 5 ($t_4$ –$t_5$): At time t = $t_4$, the main switch $S_1$ is persistently turned OFF, and the clamped diode $D_1$ turns OFF because the primary leakage current $iL_{kp}$ equals to the auxiliary inductor current $iL_{aux}$. In this mode, the input power source, the primary winding of the coupled inductor $T_r$, and the auxiliary inductor $L_{aux}$ connect in series to supply the power for the output load in the auxiliary circuit through the diode $D_2$. At the same time, the input power source, the secondary winding of the coupled inductor $T_r$, the clamped capacitor $C_1$, and the middle voltage capacitor ($C_2$) connect in series to release the energy into the HVSC through the diode $D_4$.

$$G_{VL} = \frac{V_{O1}}{V_{FC}} = \frac{1}{1-d_1+d_x} \qquad (10)$$

Mode 6 ($t_5$ –$t_6$):At time t=$t_5$, this mode begins when the main switch $S_1$ is triggered. The auxiliary inductor current $iL_{aux}$ needs time to decay to zero, the diode $D_2$ persistently conducts. In this mode, the input power source, the clamped capacitor $C_1$, the secondary winding of the coupled inductor $T_r$, and the middle-voltage capacitor $C_2$ still connect in series to release the energy into the HVSC through the diode $D_4$. Since the clamped diode $D_1$ can be selected as a low-voltage Schottky diode, it will be cut off promptly without a reverse-recovery current. Moreover, the rising rate of the primary current $iL_{kp}$ is limited by the primary-side leakage inductor $L_{kp}$. Thus, one cannot derive any currents from the paths of the HVSC, the middle-voltage circuit, the auxiliary circuit, and the clamped circuit. As a result, the main switch $S_1$ is turned ON under the condition of ZCS and this soft-switching property is helpful for alleviating the switching loss. When the secondary current $iL_S$ decays to zero, this mode ends. After that, it begins the next switching cycle and repeats the operation in mode 1.

$$G_{VL} = \frac{V_{O1}}{V_{FC}} = \frac{2}{(1-d_1)} + \frac{2}{\sqrt{(1-d_1)^2}} + \frac{2}{[\frac{8L_{aux}}{R_{O1}T_S}]} \qquad (11)$$

## IV. Experimental Results

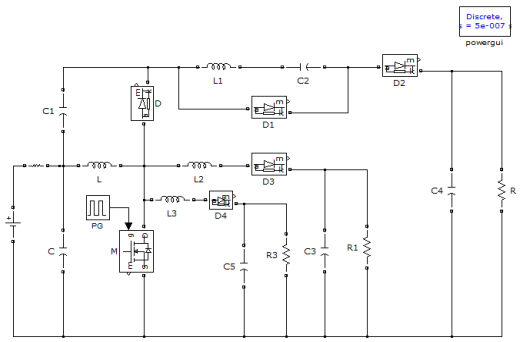


Fig.3 Simulation circuit

Digital simulation is done using MATLAB and the results are presented here. Open loop system of 12V/200V, 100 KHz dc/dc converter is shown in Fig.3.Input voltage of 12V is shown in Fig.4. The middle output voltage in open loop system is shown in Fig 5. The middle output current is shown in fig.6. The output voltage increases with the increase in the input voltage. The high output voltage in open loop system is shown in Fig.8 and high output current in open loop system is shown in Fig.9.

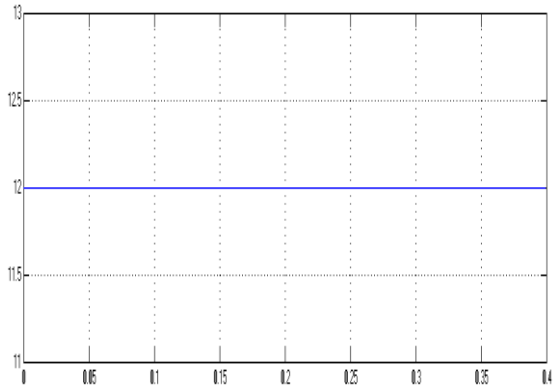


Fig.4.Input DC voltage

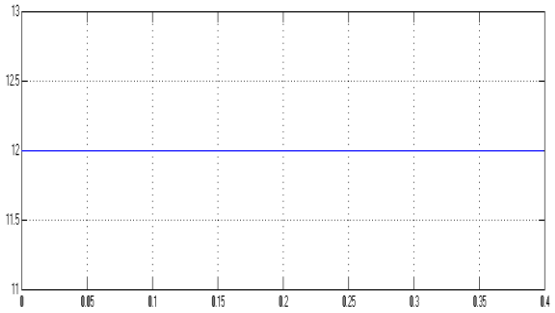


Fig.5.Middle Output Voltage

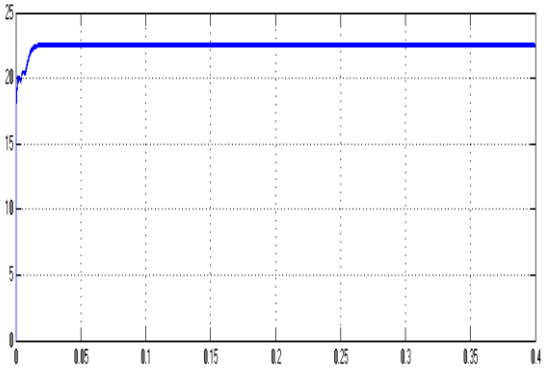


Fig.6.Middle Output Current

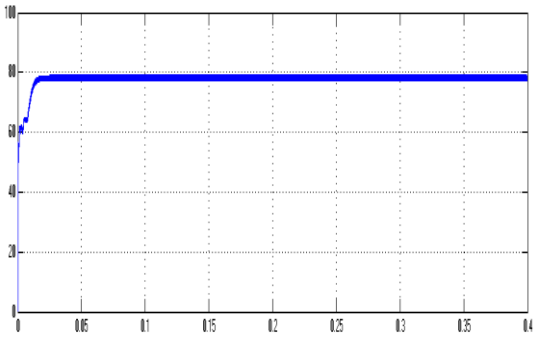

Fig.7.Middle Output Power

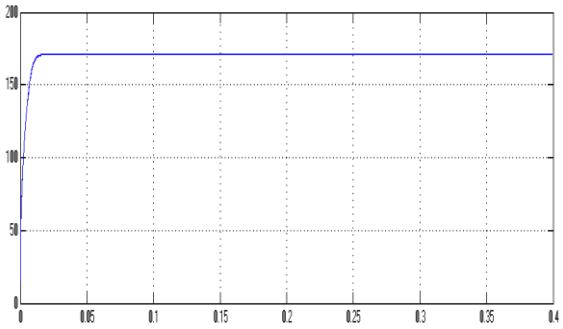

Fig.8 High Output Voltage

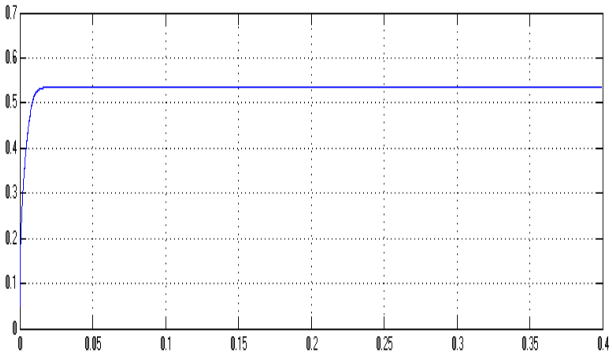

Fig.9.High Output Current

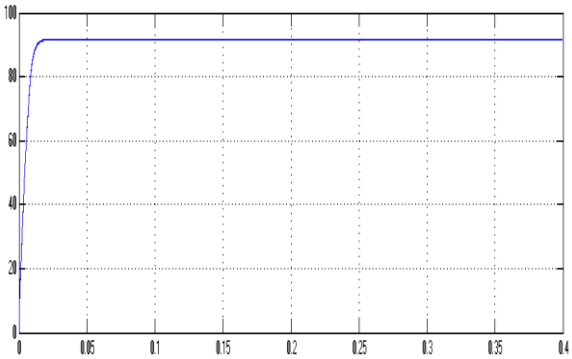

Fig.10.High Output Power

## V. Conclusion

This study has successfully developed an Embedded Controlled Multiple Output Boost Converter, and this coupled-inductor-based converter was applied well to a single-input power source plus two output terminals

composed of an auxiliary battery module and a high-voltage dc bus. This topology adopts only one power switch to achieve the objective of high-efficiency SIMO power conversion. The voltage gain can be substantially increased by using a coupled inductor. The Speed of DC drive is controlled using MOB converter. Steady State error in speed is reduced. The Basic circuit and modified circuit elements are designed using relevant equations. The simulation circuits are developed using elements of simulink library. The Simulation is successfully done and open loop / closed loop simulation results are presented. The Simulation results coincide with the theoretical results.

## REFERENCES


[1] Rong-Jong Wai, and Rou-Yong DuanW,"High Step-Up Converter With Coupled-Inductor," IEEE Trans. Power Electron., vol. 20, no. 5, pp. 1149– 1162, Sep 2005.

[2] Luciano Schuch, Cassiano Rech, Hélio Leães Hey, Hilton Abílio Gründling, Humberto Pinheiro, "Analysis and Design of a New High- Efficiency Bidirectional Integrated ZVT PWM Converter for DC-Bus and Battery-Bank Interface" IEEE Trans. Ind. Electron., vol. 42, no. 5, pp. 5154–5162, Sep/Oct 2006.

[3] Yu Chen and Yong Kang,"A Fully Regulated Dual-Output DC–DC Converter With Special-Connected Two Transformers (SCTTs Cell and Complementary Pulsewidth Modulation–PFM (CPWM-PFM)," IEEE Trans. Power Electron., vol. 25, no. 5, pp. 1149– 1162, may 2005.

[4] Mukhtiar Singh,and Ambrish Chandra,"Application of Adaptive Network-Based Fuzzy Inference System for Sensorless Control of PMSG-Based Wind Turbine With Nonlinear-Load-Compensation Capabilities," IEEE Trans. Power Electron., vol. 26, no. 1, pp. 1149– 1162, Jan 2011.

[5] Fei Gao, Benjamin Blunier, Marcelo Godoy Sim˜oes and Abdellatif Miraoui," PEM Fuel Cell Stack Modeling for Real-Time Emulation in Hardware-in-the-Loop Applications," IEEE Trans. Energy.Conv., vol. 26, no. 1, pp. 1149–1162, March 2011.

[6] Jae-Kuk Kim, Seong-Wook Choi and Gun-Woo Moon," Zero-Voltage Switching Postregulation Scheme for Multioutput Forward Converter With Synchronous Switches," IEEE Trans. Ind. Electron., vol. 58, no. 6, pp. 5154–5162,June 2011.

[7] Bangyin Liu, Shanxu Duan, and Tao Cai,"Photovoltaic DC-Building-Module-Based BIP System—Concept and Design Considerations," IEEE Trans. Power Electron., vol. 26, no. 5, pp. 1149– 1162, May 2011.

[8] Yu Chen,Yong Kang, Songsong Nie, and Xuejun Pei,"The Multiple-Output DC–DC Converter With Shared ZCS Lagging Leg," IEEE Trans. Power Electron., vol. 26, no. 8, pp. 1149– 1162, Aug 2011.

[9] Lijun Hang, Siran Wang, Yilei Gu, Wenxi Yao, and Zhengyu Lu,"High Cross-Regulation Multioutput LLC Series Resonant Converter With Magamp Postregulator," IEEE Trans. Ind. Electron., vol.58, no. 9, pp. 5154–5162, Sep 2011.

[10] Hongfei Wu, Runruo Chen, Junjun Zhang, Yan Xing, Haibing Hu, and Hongjuan Ge,"A Family of Three-Port Half-Bridge Converters for a Stand-Alone Renewable Power System," IEEE Trans. Power. Electron., vol.26, no. 9, pp. 5154–5162, Sep 2011.

[11] Annamalai Kirubakarn, Shailendra Jain and Rajesh Kumar Nema, "DSP-Controlled Power Electronic Interface for Fuel-Cell-Based Distributed Generation," IEEE Trans. Power Electron., vol. 26, no. 12, pp. 1149– 1162, Dec 2011

[12] S. D. Gamini Jayasinghe ,D. Mahinda Vilathgamuwa, and Udaya K. Madawala ,"Diode-Clamped Three-Level Inverter-Based Battery/Supercapacitor Direct Integration Scheme for Renewable Energy Systems," IEEE Trans. Power Electron., vol. 26, no. 12, pp. 1149– 1162,Dec 2011.

[13] Pradipta Patra, Amit Patra, and Neeraj Misra ,"A Single-Inductor Multiple-Output Switcher With Simultaneous Buck, Boost, and Inverted Outputs," IEEE Trans. Power Electron., vol. 27, no. 4, pp. 1149– 1162, Apr 2012.

[14] Sang-Ho Cho, Chang-Seop Kim and Sang-Kyoo Han ,"High-Efficiency and Low-Cost Tightly Regulated Dual-Output LLC Resonant Converter ," IEEE Trans. Ind. Electron., vol. 59, no. 7, pp. 5154–5162,July 2012.

[15] Ching-Tsai Pan, Ming-Chieh Chen and Ching-Ming Lai ,"A Novel Integrated DC/AC Converter With High Voltage Gain Capability for Distributed Energy Resource Systems ," IEEE Trans. Power Electron., vol. 27, no. 5, pp. 1149–1162, May 2012.

[16] A.Nami, F.Zare, A.Ghosh and F.Blaabjerg ,"Multiple-Output DC-DC converters based on diode-clamped converters configuration:Topology and control strategy," IET Power Electron.. vol.3 no.2,pp.197-208,2010.